

Measuring the underlying event at ATLAS

A. Moraes, C. Buttar and D. Clements

Department of Physics and Astronomy, Kelvin Building,
University of Glasgow, G12 8QQ, Glasgow, UK.

Abstract

In this report we investigate measurements of the underlying event in jet events at ATLAS. Reconstructed QCD jet samples in separate p_t bins produced for jet calibration (Rome samples) are used in this study. We show that reconstructed track distributions for the underlying event reproduce the MC event generator predictions.

1 Introduction

As in previous high-energy hadron colliders, soft interactions will be the dominant processes in proton-proton (pp) collisions at the LHC [1]. Thus, most particles produced at the LHC are predicted to originate from soft interactions [2]. In addition to this, soft partonic interactions are also going to be relevant to the prediction of the underlying event (UE) associated with hard processes (e.g. high- p_t QCD interaction). Accurate estimates of the UE are therefore important for the development of many physics analyses such as Higgs VBF search [3, 4].

Models describing the UE at the event generator level have been investigated in previous studies [2, 4–8]. However, investigations taking into account detector effects in reconstructed data for the ATLAS experiment [9] have not yet been done.

In this note we investigate measurements of the UE that can be made with ATLAS data. Reconstructed QCD jet samples in separate p_t bins produced for jet calibration (Rome samples [10]) are used in this study. Our aim is to assess how well reconstructed track distributions for the underlying event reproduce the MC event generator predictions.

In Sec. 2 using the CDF definition for the UE we present predictions for the LHC which highlight the large uncertainties in UE distributions, even though these are generated using models tuned to the available data [2]. Section 3 describes the reconstructed jet samples used in our analysis and in Sec. 4 we show the criteria employed to select jet events for our UE study. In Sec. 5 we discuss our results on comparisons between reconstructed track and the MC truth charged particle distributions for the UE. Finally, in Sec. 6 we present our conclusions.

2 The underlying event

In a hadronic event containing QCD jets, as illustrated in Fig. 1, the underlying event (UE) consists of all event activity except the two outgoing hard scattered jets [7]. The underlying structure of jets is not yet fully understood, and it is not clear how it should be modelled.

The event generators PYTHIA [11] and PHOJET [12] have been shown to describe properties of soft hadronic interactions, such as the UE data, reasonably well when appropriately tuned [2, 8, 13, 14]. In Ref. [2], the authors detail how the current *ATLAS tuning* for PYTHIA, which is used for the ATLAS Data Challenge productions [15], was obtained after extensive comparisons to a variety of experimental measurements done at different colliding energies. Similar work has been done by the CDF Collaboration, although their PYTHIA tuning, *CDF*

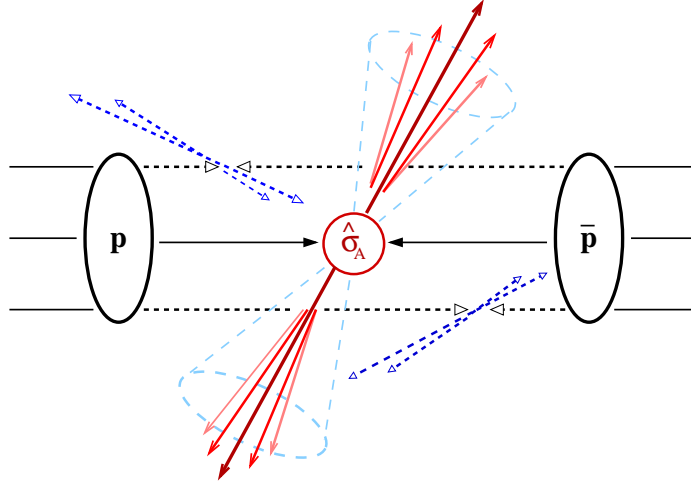


Fig. 1: Illustration of a jet produced by a hard parton-parton scattering in a $p\bar{p}$ collision.

tune A [8], is primarily based on the description of the UE in jet events measured for proton-antiproton ($p\bar{p}$) at centre-of-mass energy $\sqrt{s} = 1.8$ TeV [7].

Based on the CDF study presented in Ref. [7], using their definition for the UE, i.e. the angular region in ϕ (the azimuthal angle) which is transverse to the leading charged particle jet, one can generate LHC predictions for the UE. Figure 2 shows PYTHIA6.214 - ATLAS [2] and CDF tune A [8], and PHOJET1.12 [2, 12] predictions for the average charged particle multiplicity in the UE for jet events in pp collisions at the LHC (charged particles with transverse momentum $p_t > 0.5$ GeV and pseudorapidity $|\eta| < 1$). The distributions generated by the three models are considerably different. Excepting the events with $P_{t_{\text{jet}}} \lesssim 3$ GeV, PYTHIA6.214 - ATLAS generates greater multiplicity in the UE than the other models shown in Fig. 2.

A close inspection of predictions for the UE given in Fig. 2, shows that the average charged particle multiplicity in the UE for leading jets with $P_{t_{\text{jet}}} > 10$ GeV reaches a plateau at ~ 6.5 charged particles according to PYTHIA6.214 - ATLAS, ~ 5 for CDF tune A and ~ 3.0 according to PHOJET1.12. Expressed as particle densities per unit $\eta - \phi$, where the UE phase-space is given by $\Delta\eta\Delta\phi = 4\pi/3$ [7, 8], these multiplicities correspond to 1.56, 1.19 and 0.72 charged particles per unit $\eta - \phi$ ($p_t > 0.5$ GeV), as predicted by PYTHIA6.214 - ATLAS, CDF tune A and PHOJET1.12, respectively.

Compared to the underlying event distributions measured by CDF at 1.8 TeV [7], PYTHIA 6.214 - ATLAS indicates a plateau rise of $\sim 200\%$ at the LHC while PYTHIA6.214 - CDF tune A predicts a rise of $\sim 100\%$ and PHOJET1.12 suggests a much smaller rise of $\sim 40\%$.

The comparison shown in Fig. 2 indicates that there are large uncertainties in predictions for the UE at the LHC. In the next sections, we shall investigate how the reconstructed UE data from ATLAS compares to predictions at the event generator level. This will allow us to investigate if measurements accurate enough to allow us to identify which model agrees best to the observed UE data can be made at the start up of ATLAS.

3 Reconstructed jet samples

The ATLAS simulation and reconstruction software has been intensively tested and updated in the past few years [16, 17]. Large samples of simulated physics signals and backgrounds have

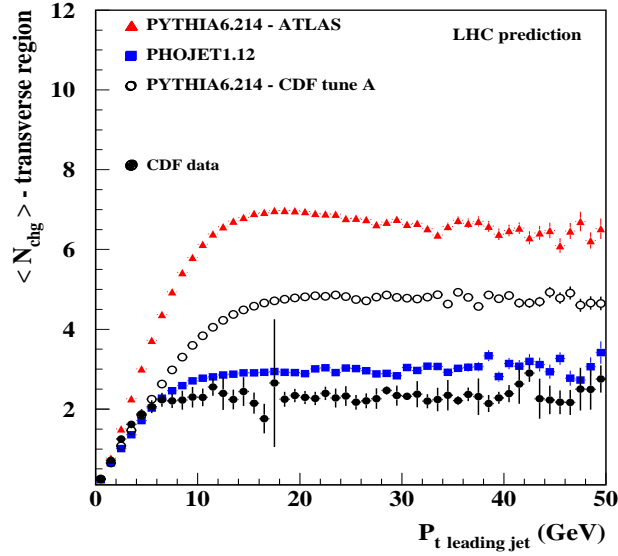


Fig. 2: PYTHIA6.214 - ATLAS and CDF tune A and PHOJET1.12 predictions for the average multiplicity in the UE for LHC pp collisions.

recently been prepared for analysis which focused on fully simulated and reconstructed events assuming the initial ATLAS geometry [10]. Among the produced samples, there are QCD jet samples which were produced in 8 p_t bins spanning a jet p_t range of $p_t^{\text{lead. jet}} > 17$ GeV.

Reconstructed jet samples [10]	Leading jet p_t range
J1: rome.003034.reco.J1_Pt_17_35._xxxxx.pool.root	$17 < p_t < 35$ GeV
J2: rome.003035.reco.J2_Pt_35_70._xxxxx.pool.root	$35 < p_t < 70$ GeV
J3: rome.003036.reco.J3_Pt_70_140._xxxxx.pool.root	$70 < p_t < 140$ GeV
J4: rome.003037.reco.J4_Pt_140_280._xxxxx.pool.root	$140 < p_t < 280$ GeV
J5: rome.003038.reco.J5_Pt_280_560._xxxxx.pool.root	$280 < p_t < 560$ GeV
J6: rome.003039.reco.J6_Pt_560_1120._xxxxx.pool.root	$560 < p_t < 1120$ GeV
J7: rome.003040.reco.J7_Pt_1120_2240._xxxxx.pool.root	$1120 < p_t < 2240$ GeV
J8: rome.003041.reco.J8_Pt_2240._xxxxx.pool.root	$p_t > 2240$ GeV

Table 1: Reconstructed QCD jet samples assuming the initial ATLAS geometry - *Rome samples*.

Table 1 shows the reconstructed jet samples which were produced assuming the initial ATLAS layout. The samples used in our analysis were reconstructed using ATHENA 10.0.1 [17]. PYTHIA6.226 with the ATLAS tuning [2] was the event generator used in the production of these samples [18]. The simulation settings used can be found in Ref. [19].

In this work, 40,000 reconstructed events from samples J1, J2, J3, J4 and J5 were used, while for the remaining samples, J6, J7 and J8, 20,000 reconstructed events were investigated.

4 Selecting jet events

Assuming that LHC events have been triggered, reconstructed and stored on disk, or in our case, simulated and reconstructed, then selecting suitable jet events is the first step to the study of the underlying event associated to jet production.

We use multi-jet samples and require jets detected in the precision region of the ATLAS detector, i.e. $|\eta_{jet}| < 2.5$ [9]. The jet E_T cut is 10 GeV, which is the standard cut used in the ATHENA release 10.0.1. In this analysis, the cone jet algorithm was used as our clustering algorithm to identify jets. Two cone-radius sizes were investigated: $R=0.4$ and 0.7 .

Figure 3 shows jet multiplicity distributions from samples J4 and J6 (see Table 1) for two cone-radius sizes: $R=0.4$, Figs. 3(a) and (b), and $R=0.7$, Figs. 3(c) and (d). In Fig. 3 we compare multiplicities of reconstructed and *MC truth* jets (i.e. event generator level). Note that some of the jets seen in the MC truth distributions are not present in the reconstructed jet distributions. However, as can be seen by comparing Figs. 3(a) and (b) to 3(c) and (d), the reconstructed jet distributions agree better to the MC truth jet distributions for the smaller cone-radius size of $R=0.4$. Although here we show only results for comparisons of two jet samples (J4 and J6), similar results are seen for the other samples we investigated.

As seen in Fig. 3 not all jets are reconstructed and, based on the calorimeter performance [9], the lost jets are mainly going to be low E_T jets. However, in our UE analysis, which is inspired by CDF measurements such as those shown in Refs. [7, 20, 21], it is rather more essential to describe the leading jet with as much accuracy as possible, since its centroid coordinates are used to define the UE. How efficiently calorimeters measure lower E_T jets is not going to be an issue in this particular analysis.

Figure 4 displays leading jet E_T distributions for reconstructed and MC truth jets. The jet distributions were obtained from the J3 sample. The leading jet is defined as the highest E_T calorimeter jet in the selected event. Reconstructed and MC truth distributions are in good agreement for both cone-radius sizes shown in Fig. 4. Leading jet distributions from the other jet samples produce similar results to those shown for J3.

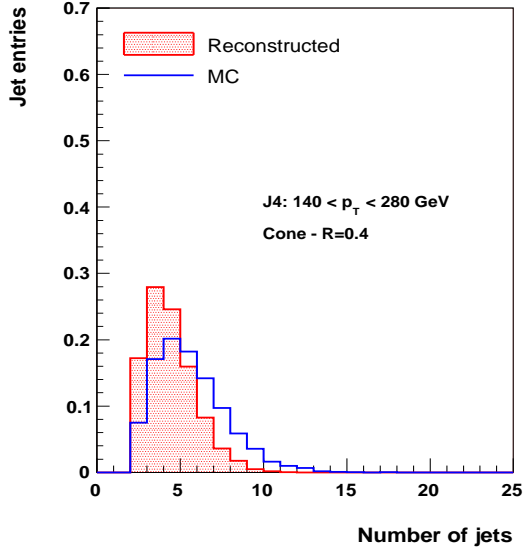
From the comparisons shown in Figs. 3 and 4 we see that reconstructed and MC truth jets agree for the leading calorimeter jet E_T spectrum, but not for distributions of the total jet multiplicity in the event. Regarding underlying event measurements in QCD jet events, these results indicate that a definition for the underlying event similar to that applied in recent CDF studies [7, 20, 21] can be employed to analyse ATLAS data.

5 Selecting the underlying event

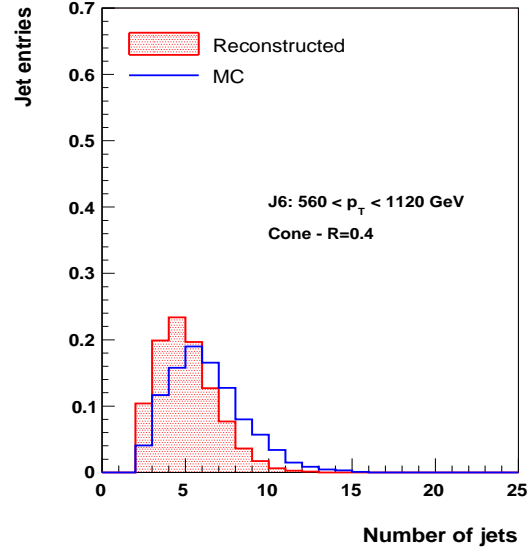
The study of the underlying event (UE) requires, first, the identification of events with the hard process of interest, or in this analysis in particular, jet events ($N_{jet} > 1$, $|\eta_{jet}| < 2.5$, jet $E_T > 10$ GeV). In jet events, the highest E_T jet, or leading calorimeter jet, is used to define the event and, hence, the UE.

Three regions are defined in terms of the azimuthal angle between tracks (reconstructed), or charged particles (MC generator level), and the leading jet. This angular difference is given by $\Delta\phi = \phi_{track} - \phi_{ljet}$. The region $|\Delta\phi| < 60^\circ$ is referred to as toward the leading jet and the region $|\Delta\phi| > 120^\circ$ is called away from the leading jet. The region transverse to the leading jet is defined by $60^\circ < |\Delta\phi| < 120^\circ$, and is used to study the underlying event. The event regions defined by $\Delta\phi$ are illustrated in Fig. 5.

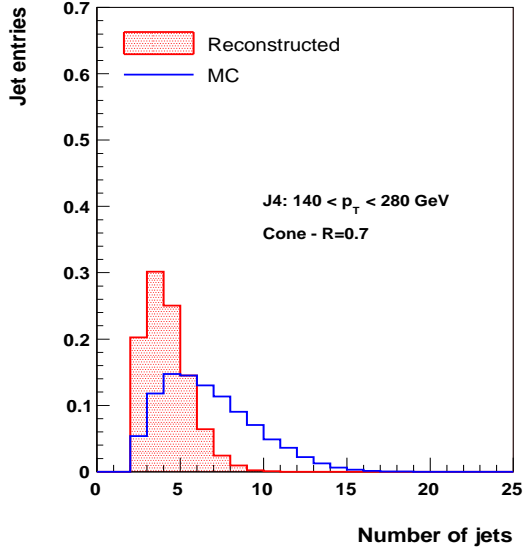
In this analysis, reconstructed tracks are selected within the ATLAS pseudorapidity ac-



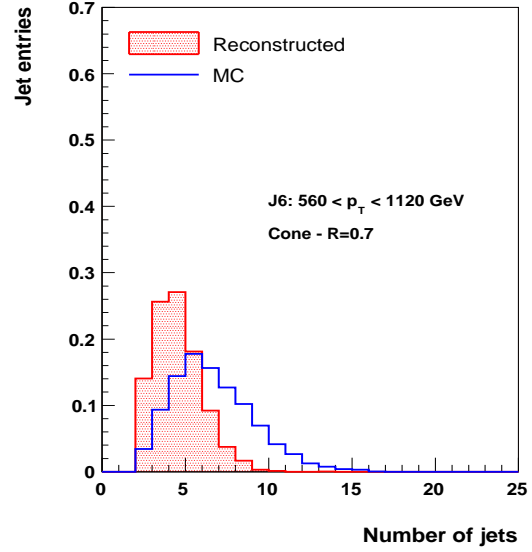
(a)



(b)



(c)



(d)

Fig. 3: Number of jet distributions: reconstructed vs. MC truth. Cone jet finder with R=0.4 (a) sample J4 and (b) J6. For R=0.7 (c) sample J4 and (d) J6.

ceptance $|\eta_{track}| < 2.5$ [9] and with transverse momentum of $p_t^{track} > 1$ GeV. Figure 6 displays the average track multiplicity, $\langle N_{track} \rangle$ (Fig. 6(a)), and average track P_t sum in the transverse region, i.e. the UE (Fig. 6(b)). In these plots, the leading jets were identified by using a cone-jet finder with a cone radius R=0.7.

The plots shown in Fig. 6 include information from reconstructed jet samples from J1 to J6, as listed in Table 1. Samples J7 and J8 were not included because of prohibitively large

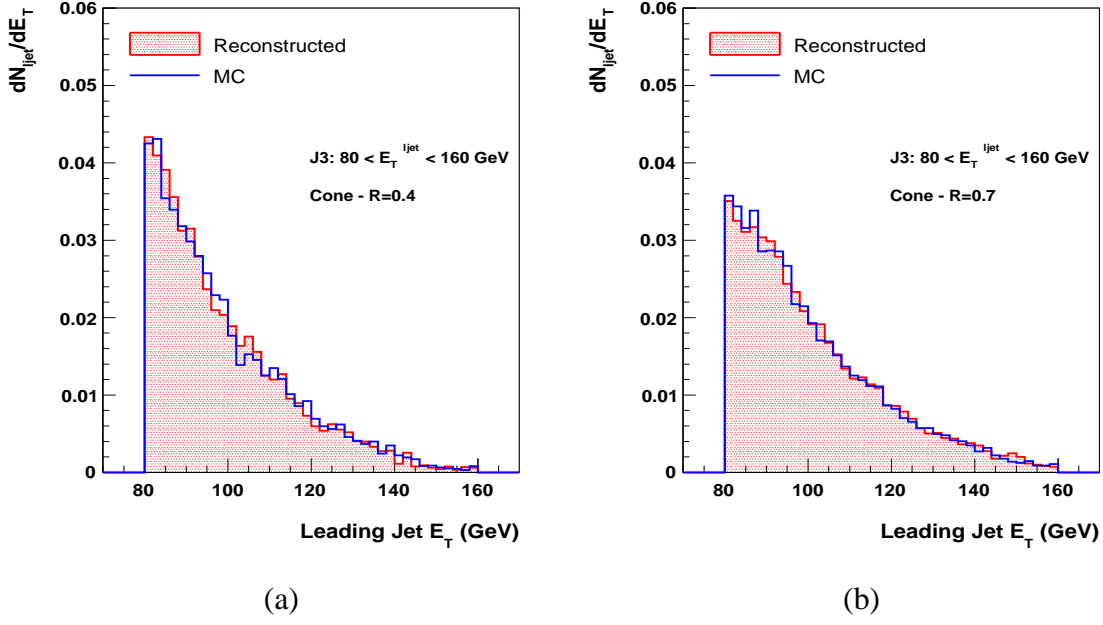


Fig. 4: Leading jet E_T distribution: reconstructed vs. MC truth. (a) cone jet finder with $R=0.4$ and (b) $R=0.7$.

statistical uncertainties in UE distributions for very high- E_T jets. Note that, even though we have only several tens of thousands of jet events, we are able to combine the information from different jet- E_T bins and plot UE distributions spanning a range of $20 < \text{lead. jet } E_T < 1000$ GeV.

Figure 7 shows UE distributions for reconstructed tracks compared to distributions obtained from MC truth charged particles. Leading jets were identified with a cone-jet finder with $R=0.7$. MC truth charged particles were selected with the same kinematic cuts used for reconstructed tracks, i.e. $|\eta_{\text{MC chg. part.}}| < 2.5$, $p_t^{\text{MC chg. part.}} > 1$ GeV and $60^\circ < |\Delta\phi| < 120^\circ$ where $\Delta\phi = \phi_{\text{MC chg. part.}} - \phi_{\text{MC ljet}}$. The reconstructed distributions for both $\langle N_{\text{track}} \rangle$, Fig. 7(a), and $\langle P_{t \text{ sum}}^{\text{track}} \rangle$, Fig. 7(b), reproduce those from MC truth charged particles. The ratios “reconstructed/MC truth”, for both $\langle N_{\text{track}} \rangle$ and $\langle P_{t \text{ sum}}^{\text{track}} \rangle$, indicate that distributions from reconstructed tracks are in good agreement with the MC truth distributions for most of the jet E_T range investigated. A noticeable difference is seen for the lower E_T jet sample, corresponding to jet sample J1. Statistical uncertainties are also clearly noticeable, especially at the highest E_T end of the jet samples used in this study.

Taking into account that we are looking at a wide jet E_T range (the widest ever used in UE analysis) and that ratios between reconstructed and MC truth distributions are, in most of the E_T range investigated, not far from 1, the reconstructed information should provide a good measurement of the UE. Uncertainties arising from conversion effects and secondary decays have not been investigated here and, when included in our UE analysis, are likely to improve the quality and accuracy of such measurements. Other improvements can be made with larger statistical samples and by understanding the lower E_T jet reconstruction efficiency.

Figure 8 shows, again, UE distributions for reconstructed tracks compared to distributions obtained from MC truth charged particles. In this case, however, the cone-jet algorithm was

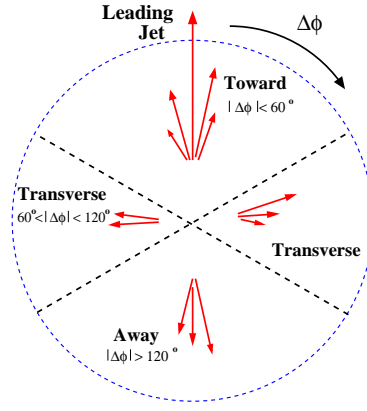


Fig. 5: Event regions defined in terms of the azimuthal angle between tracks (or charged particles) and the leading calorimeter jet, $\Delta\phi = \phi_{\text{track}} - \phi_{\text{ljjet}}$.

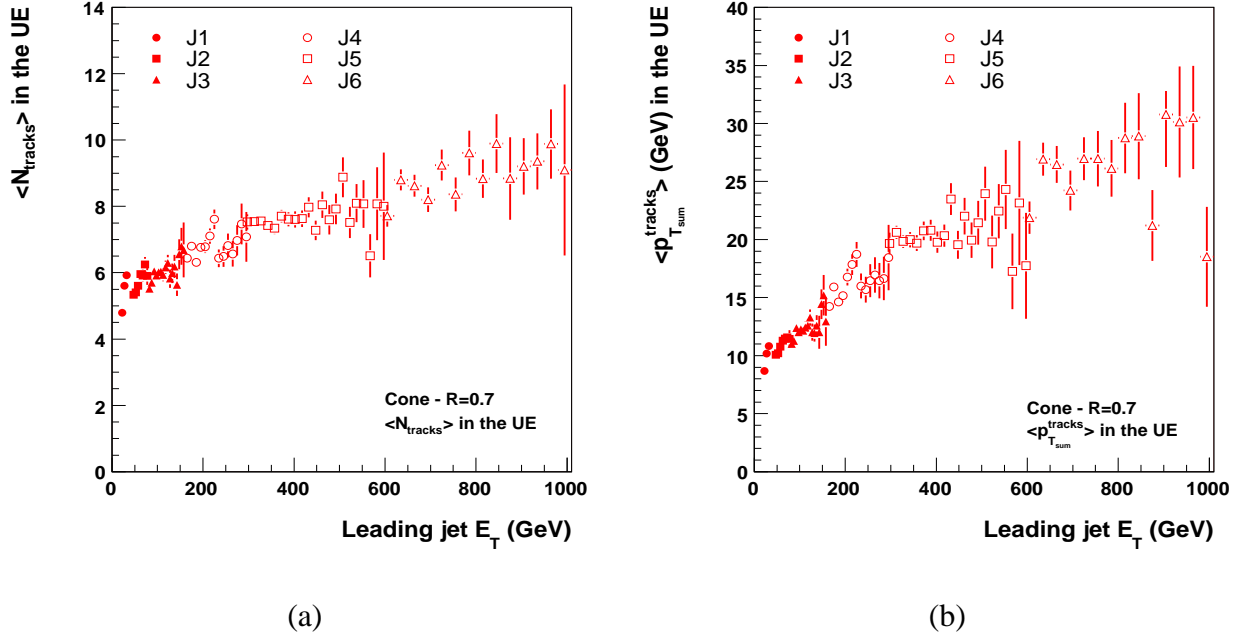


Fig. 6: UE distributions: (a) Average track multiplicity in the transverse region and (b) average track P_t sum in the transverse region.

used with a cone radius $R=0.4$. The results are similar to those seen for $R=0.7$, as shown in Fig. 7. Once again, the ratios “reconstructed/MC truth”, for both $\langle N_{\text{track}} \rangle$ and $\langle P_{t \text{ sum}}^{\text{track}} \rangle$, indicate that distributions from reconstructed tracks are in good agreement to the MC truth distributions. An inspection of the plots displayed in Figs. 7 and 8 also suggests that the UE predictions for $\langle N_{\text{track}} \rangle$ and $\langle P_{t \text{ sum}}^{\text{track}} \rangle$ are independent of the cone radius used to select the leading jet.

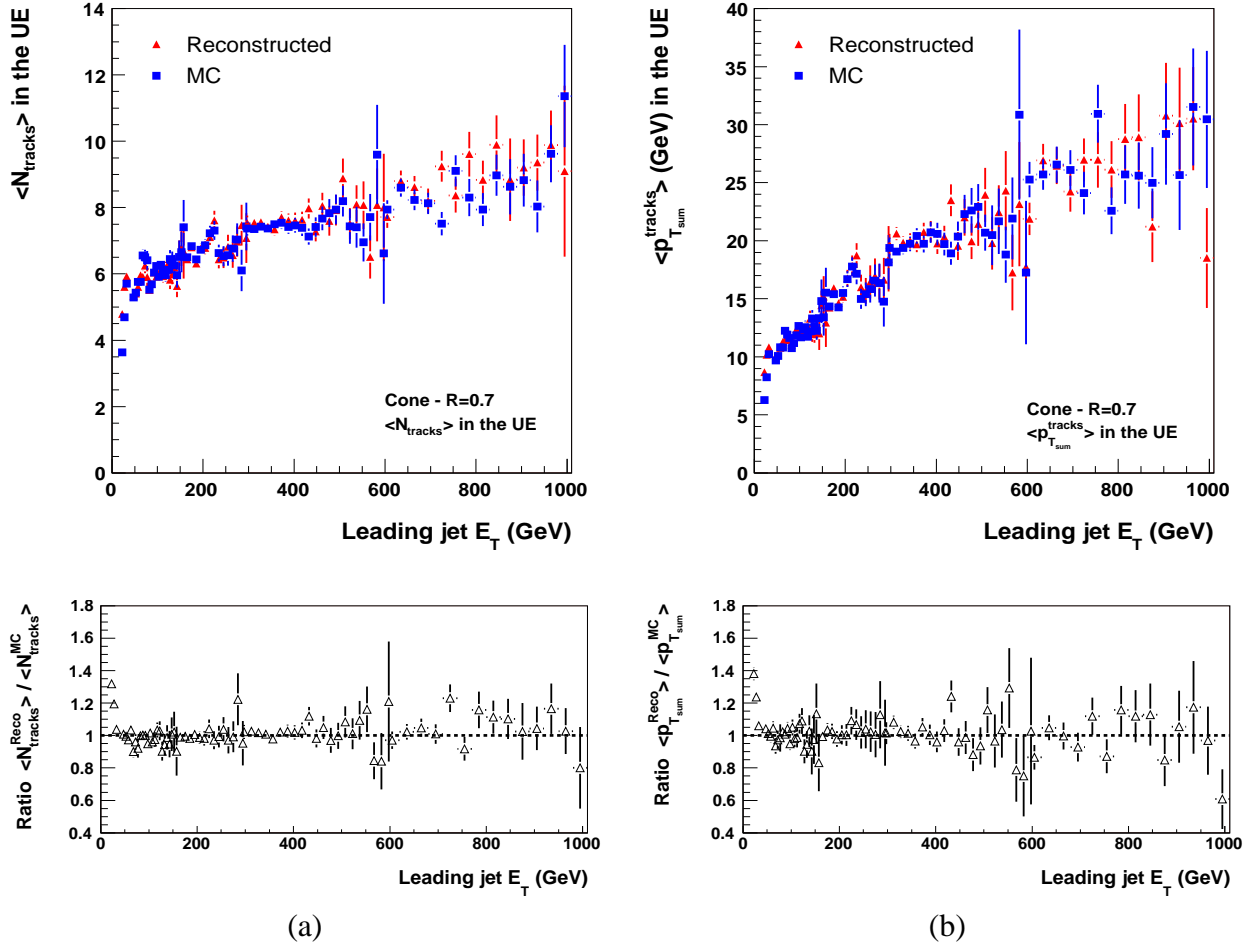


Fig. 7: UE distributions: reconstructed vs. MC truth. (a) $\langle N_{\text{track}} \rangle$ and (b) $\langle p_{t \text{ sum}}^{\text{track}} \rangle$

6 Conclusion

In this note we have investigated measurements of general properties of the UE at ATLAS. Reconstructed QCD jet samples in separate p_t bins (Rome samples [10]) were used in this study in order to assess how well reconstructed track distributions for the UE reproduce the MC event generator predictions.

We have verified that reconstructed track distributions for both $\langle N_{\text{track}} \rangle$ in the UE, Figs. 7(a) and 8(a), and $\langle p_{t \text{ sum}}^{\text{track}} \rangle$, Figs. 7(b) and 8(b), reproduce those from MC truth charged particles. The ratios “reconstructed/MC truth”, for both $\langle N_{\text{track}} \rangle$ and $\langle p_{t \text{ sum}}^{\text{track}} \rangle$, show that reconstructed track distributions are in good agreement to the MC truth distributions for most of the jet E_T range investigated, i.e. UE distributions spanning a leading jet E_T range of $20 < E_T < 1000$ GeV.

The lower E_T jet sample, corresponding to jet sample J1 (Table 1), shows UE distributions with the largest disagreement between reconstructed track and MC truth distributions. This needs to be further investigated. Statistical uncertainties are also clearly noticeable, and a more detailed quantitative study would, therefore, require larger statistical jet samples.

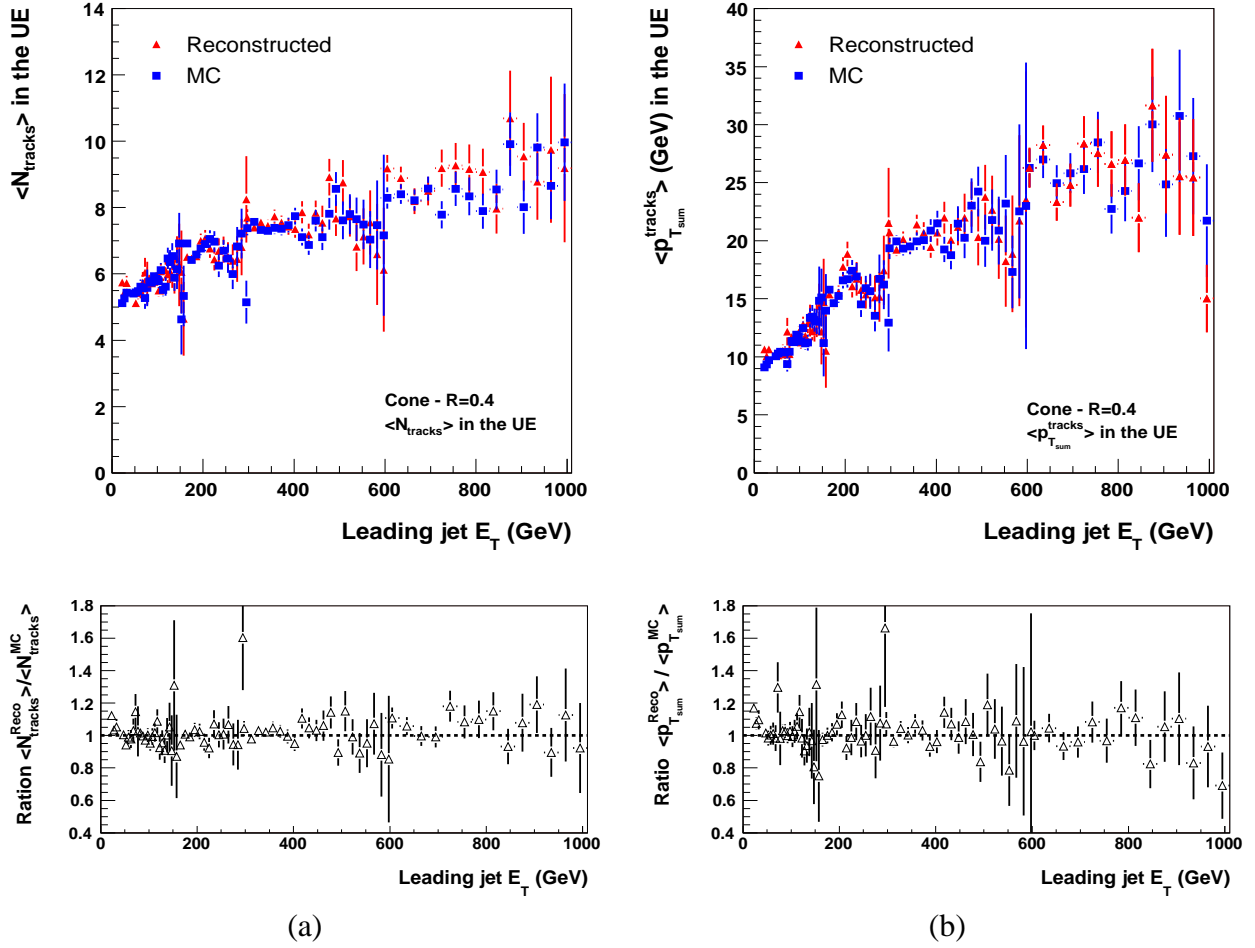


Fig. 8: UE distributions for leading jets identified with a cone-jet finder of radius $R=0.4$: reconstructed vs. MC truth. (a) $\langle N_{track} \rangle$ and (b) $\langle p_{t\text{sum}}^{track} \rangle$

As pointed out before, uncertainties arising from conversion effects and secondary decays have not been included in this study and, when added to our UE analysis, are likely to improve the quality and accuracy of such measurements. Uncertainties in the detection of the leading calorimeter jet have not been included either. However, by limiting our leading jet selection to the ATLAS precision region ($|\eta_{ljet}| < 2.5$) [9] we hoped to minimise any considerable contributions coming from systematic uncertainties related to the leading jet selection.

The results shown in Figs. 7 and 8 suggest that the UE predictions for $\langle N_{track} \rangle$ and $\langle p_{t\text{sum}}^{track} \rangle$ measurements are independent of the cone radius size used in the cone-jet algorithm.

Considering that we are looking at the widest jet E_T range ever used in UE analysis and that ratios between reconstructed and MC truth distributions are, in most of the E_T range investigated, not far from unity, we expect from this preliminary study that the ATLAS reconstructed information will provide a good measurement of the UE.

Based on the comparisons shown in this note, we expect UE measurements to be accurate enough to allow the identification of which physics model describes best the properties of soft hadronic physics in the UE. Moreover, assuming that pre-scaled jet triggers will be made

available at ATLAS in addition to the single jet triggers already planned, there will be enough statistics in the first few days of data taking (low luminosity) not only to reproduce the simulated results presented here, but certainly will also improve them statistically.

References

- [1] *The Large Hadron Collider, Conceptual Design*, October 1995. CERN-AC-95-05 LHC.
- [2] A. Moraes, C. Buttar and I. Dawson, p. 46 (2005). ATL-PHYS-PUB-2005-007.
- [3] S. Asai *et al.*, Eur. Phys. J. **C32 (S2)**, 19 (2004).
- [4] C. Buttar, D. Clements, I. Dawson and A. Moraes, Acta Phys. Polon. **B35**, 433 (2004).
- [5] I. Dawson, C. Buttar and A. Moraes, Czech. J. Phys. **54**, A221 (2004).
- [6] M. Dobbs *et al.*, *The QCD / SM working group: summary report*, March 2004. Report of the Working Group on Quantum Chromodynamics and the Standard Model. Contributed to 3rd Les Houches Workshop: Physics at TeV Colliders, Les Houches, France, 26 May-6 Jun 2003 (hep-ph/0403100).
- [7] T. Affolder *et al.*, Phys. Rev. **D65**, 092002 (2002).
- [8] R. Field, *Min-Bias and the Underlying Event at the Tevatron and the LHC*, October 2002. (talk presented at the Fermilab ME/MC Tuning Workshop, Fermilab).
- [9] *ATLAS Detector and Physics Performance, Technical Design Report*, May 1999. CERN/LHCC/99-14.
- [10] *List of Rome samples*, June 2005. ATLAS list of samples Wiki: <https://uimon.cern.ch/twiki/bin/view/Atlas/RomeListOfSamples>.
- [11] T. Sjostrand, L. Lonnblad and S. Mrenna, *PYTHIA 6.2 - Physics and Manual*, August 2001. Hep-ph/0108264.
- [12] R. Engel, *PHOJET manual (program version 1.05)*, June 1996.
- [13] T. Sjostrand and M. van Zijl, Phys. Rev. D **36**, 2019 (1987).
- [14] R. Engel, *Hadronic Interactions of Photons at High Energies*, 1997. Siegen (PhD Thesis).
- [15] *Physics Generation for Atlas Data Challenges*, 2004/2005. Job options for event generators: <http://www-theory.lbl.gov/%7Eianh/dc/>.
- [16] *ATLAS Computing Technical Design Report*, June 2005. ATLAS TDR-017, CERN-LHCC-2005-022.
- [17] *Atlas Software*, 2005. Software project domains: <http://atlas.web.cern.ch/Atlas/GROUPS/SOFTWARE/OO/Applications/>.
- [18] *Generator Job Options for Rome*, 2005. ATLAS CVS: <http://atlassw1.phy.bnl.gov/lxr/source/atlas/Generators/GeneratorOptionsRome/share/>.

- [19] *Simulation Job Options for Rome*, 2005. ATLAS CVS:
<http://atlassw1.phy.bnl.gov/lxr/source/atlas/Simulation/SimulationOptionsRome/>.
- [20] *Jet Evolution and the Underlying Event in Run 2*, 2003. CDF - QCD Run II results:
<http://www-cdf.fnal.gov/physics/new/qcd/run2/ue/chgjet/index.html>.
- [21] D. Acosta *et al.*, Phys. Rev. **D70**, 072002 (2004).